JOURNAL OF BACTERIOLOGY, Feb. 2008, p. 1097–1107 Vol. 190, No. 3
0021-9193/08/$08.00+0 doi:10.1128/JB.00516-07

Campylobacter jejuni Biofilms Up-Regulated in the Absence of the Stringent Response Utilize a Calcofluor White-Reactive Polysaccharide▽

Meghan K. McLennan,[1]† Danielle D. Ringoir,[1]† Emilisa Frirdich,[1]‡ Sarah L. Svensson,[1]‡ Derek H. Wells,[2] Harold Jarrell,[3] Christine M. Szymanski,[3] and Erin C. Gaynor[1]*

Department of Microbiology and Immunology, University of British Columbia, Vancouver, British Columbia, Canada[1]; Division of Infectious Diseases, University of California San Francisco, San Francisco, California[2]; and Institute for Biological Sciences, National Research Council, Ottawa, Ontario, Canada[3]

Received 4 April 2007/Accepted 30 October 2007

The enteric pathogen *Campylobacter jejuni* is a highly prevalent yet fastidious bacterium. Biofilms and surface polysaccharides participate in stress survival, transmission, and virulence in *C. jejuni*; thus, the identification and characterization of novel genes involved in each process have important implications for pathogenesis. We found that *C. jejuni* reacts with calcofluor white (CFW), indicating the presence of surface polysaccharides harboring β1-3 and/or β1-4 linkages. CFW reactivity increased with extended growth, under 42°C anaerobic conditions, and in a Δ*spoT* mutant defective for the stringent response (SR). Conversely, two newly isolated *dim* mutants exhibited diminished CFW reactivity as well as growth and serum sensitivity differences from the wild type. Genetic, biochemical, and nuclear magnetic resonance analyses suggested that differences in CFW reactivity between wild-type and Δ*spoT* and *dim* mutant strains were independent of well-characterized lipooligosaccharides, capsular polysaccharides, and *N*-linked polysaccharides. Targeted deletion of *carB* downstream of the *dim13* mutation also resulted in CFW hyporeactivity, implicating a possible role for carbamoylphosphate synthase in the biosynthesis of this polysaccharide. Correlations between biofilm formation and production of the CFW-reactive polymer were demonstrated by crystal violet staining, scanning electron microscopy, and confocal microscopy, with the *C. jejuni* Δ*spoT* mutant being the first SR mutant in any bacterial species identified as up-regulating biofilms. Together, these results provide new insight into genes and processes important for biofilm formation and polysaccharide production in *C. jejuni*.

Campylobacter jejuni is the leading cause of bacterial gastroenteritis in the developed world, surpassing *Escherichia coli* and *Salmonella* and *Shigella* spp. combined (2). Current reports suggest that campylobacteriosis accounts for 5 to 15% of all diarrheal illnesses worldwide, affecting ~1% of the North American, United Kingdom, and Australian populations each year (1, 55, 85). These are likely underestimates, as a significant number of cases go unreported. Complications arising from *C. jejuni* infection include reactive arthritis and Guillain-Barré syndrome (GBS), a neuropathological disorder characterized by acute ascending bilateral paralysis (54). GBS is thought to be due to molecular mimicry, whereby antibodies generated against *C. jejuni* lipooligosaccharide (LOS) attack peripheral nerve gangliosides harboring similar structures (87).

C. jejuni infection is a natural zoonotic organism, residing asymptomatically as part of the normal flora in many animal species (8, 12, 19, 84). The major source of sporadic infection is thought to be the consumption of undercooked contaminated poultry or cross-contamination of other food products with raw poultry juice (50). Larger-scale outbreaks have been attributed to the consumption of unpasteurized milk and fecally contaminated water sources (49, 50). Thus, despite having fastidious laboratory growth requirements, *C. jejuni* must possess mechanisms allowing it to survive a range of in vivo and ex vivo (i.e., outside of an animal host) conditions.

One such survival mechanism is the *C. jejuni* stringent response (SR), which we recently identified as important both for the virulence-related phenotypes of cell invasion and intracellular survival and for transmission-related phenotypes including growth and survival in suboptimal CO_2 and O_2 environments (26). The *C. jejuni* SR is regulated by *spoT*, which encodes an enzyme that catalyzes the synthesis and hydrolysis of guanosine tetraphosphate (ppGpp), an alarmone that mediates the SR by binding RNA polymerase and altering gene expression. Other gram-negative alpha- and epsilonproteobacteria as well as most gram-positive organisms likewise utilize a single bifunctional ppGpp synthetase/hydrolase (51, 53, 82). In contrast, gram-negative gammaproteobacteria utilize two ppGpp biosynthetic genes, *relA* and *spoT* (51).

The *C. jejuni* SR exhibits several other differences from the SRs of other well-studied bacteria. For instance, a *C. jejuni* Δ*spoT* mutant did not exhibit increased sensitivity to several predicted stresses, including osmotolerance, serum sensitivity, and mouse and chick colonization (26; also E. Gaynor, unpublished data), which were stresses affecting SR mutants in other bacteria (56, 61). Furthermore, many other gram-negative SRs signal through the stationary-phase sigma factor *rpoS*, which is absent from *C. jejuni.* These data suggest the existence of stress response pathways in *C. jejuni* that function independently of

* Corresponding author. Mailing address: Department of Microbiology and Immunology, University of British Columbia, 2350 Health Sciences Mall, Vancouver, British Columbia, Canada V6T 1Z3. Phone: (604) 822-2710. Fax: (604) 822-6041. E-mail: egaynor@interchange.ubc.ca.

† M.K.M. and D.D.R. contributed equally to this work.

‡ E.F. and S.L.S. contributed equally to this work.

▽ Published ahead of print on 9 November 2007.

SpoT and complement the absence of a classical stationary-phase response.

Although much of *C. jejuni* biology is poorly understood compared to model organisms, *C. jejuni* surface polysaccharides and glycosylation pathways have been shown to play important roles in both virulence and stress survival (7, 28, 66, 69). A significant proportion of the *C. jejuni* genome is dedicated to known and putative polysaccharide synthesis and modification genes (22, 23, 60). Polysaccharide structures characterized to date include LOS, *N*-linked glycoproteins, capsular polysaccharides (CPS), and *O*-linked flagellar glycoproteins (69, 73), many of which are involved in important functions including motility, virulence, colonization, serum resistance, ex vivo survival, and immune evasion (7, 37, 69).

Calcofluor white (CFW) binds β1-3 and β1-4 carbohydrate linkages and fluoresces under long-wave UV light (62, 83). It has been used to study surface polysaccharides in a variety of organisms, some of which correspond to exopolysaccharides (EPSs) involved in stress survival and biofilm formation (40, 41, 67, 82, 89). Biofilms are now appreciated as a critical lifestyle stage for many bacteria and are important for survival in many environments, including those associated with pathogenesis (25, 40, 45). The initial bacterial attachment event is complex and influenced by many variables, while biofilm maturation involves the development of slow-growing protective communities characterized by low metabolic activity and encasement in a matrix of extracellular polymeric substances (13, 20, 24, 45). EPSs are an important component of the biofilm matrix; however, their structures and synthesis mechanisms can differ significantly between bacteria (20). For example, *E. coli* and *S. enterica* serovar Typhimurium utilize cellulose and colanic acid as crucial components of their extracellular matrices (13, 40, 48, 67, 89); *E. coli* also utilizes poly-β-GlcNAc polymers, as do *Bordetella* spp. (59, 80, 81), and *Staphylococcus epidermidis* and *S. aureus* utilize polysaccharide intercellular adhesin or poly-*N*-acetylglucosamine polymers (20, 44, 46). Intraspecies variability in both gene content and polysaccharide expression between *Pseudomonas aeruginosa* strains has also been observed (13).

For *C. jejuni*, biofilms have only recently begun to be characterized at a molecular genetic level (35, 36, 63, 65) but have been hypothesized as important both for in vivo colonization, as proposed for *Salmonella* (40, 88), and for transmission and ex vivo survival, such as on the nipples of chicken water bottle feeders (76, 88). Interestingly, all SR mutants in other bacteria published to date are defective for biofilm formation, indicating a relationship between these two stress response phenomena (10, 30, 42, 71). In this study, we provide evidence that *C. jejuni* produces a CFW-reactive polysaccharide that appears to be distinct from other surface polysaccharides and that production of this polysaccharide correlates with biofilm formation in the wild type (WT) and in Δ*spoT* and two novel *dim* (CFW-hyporeactive) mutant strains. This study also provides additional insight into *C. jejuni* serum stress survival and general aspects of biofilm formation, identifies new genes potentially involved polysaccharide production, and is the first demonstration of an SR mutant with a hyperbiofilm phenotype.

TABLE 1. Primers used in this study

Primer name	Sequence (5′→3′)
>H3up	TCATATCCTTTTTTTAGATTTAAG
H3down	CACTTTCCCTGTTTCTATGATACC
N	CCAGTTCCCATCTATTTTGTCAC
S	GCTTTTTCACAGCATAACTGGAC
gne-L2	TGAAAATTCTTATTAGCGGTGGT
gne-R2	CCCAATCAAAAGCAGATTACAA
carB-4fL1	GCCTCGAGGAACTCAAGCCGCAAAGACT
carB-4fR1	GCGAATTCAACCACACCACTTCCAGCAC
carB-4fL2	GCGGATCCAAAAACCGCAGATATTGCTTTA
carB-4fR2	GCGAGCTCGCTTTACATATTCTGCAGCGATT

MATERIALS AND METHODS

Bacterial growth conditions and strains. Unless otherwise stated, all *C. jejuni* strains were grown on Mueller-Hinton (MH) agar or broth (Oxoid) supplemented with trimethoprim (T) and vancomycin (V) (MH-TV) at 37°C in 6% O_2-12% CO_2 (microaerobic) conditions generated using a trigas incubator (Heraeus) or the Oxoid Campygen system. *E. coli* cultures were grown in Luria-Bertani (LB) broth or on LB agar in atmospheric conditions at 37°C. Antibiotic concentrations were as follows: ampicillin, 50 μg/ml; chloramphenicol (Cm), 25 μg/ml; kanamycin (Kan), 50 μg/ml; T, 5 μg/ml; and V, 10 μg/ml. *C. jejuni* strain 81-176, isolated from a raw milk outbreak (39), was used as the WT strain for all experiments. The 81-176 Δ*spoT* mutant was previously described (26). An 81-176 UDP-GlcNAc/Glc4 epimerase (*gne*) mutant was generated by PCR amplifying the *gne*::Kan^r disruption locus from a *C. jejuni* 11168 Δ*gne* mutant (11) by use of primers gne-L2 and gne-R2 (Table 1). The *gne*::Kan^r construct was ligated into pGEM (Promega) and introduced into WT 81-176 as a suicide vector by electroporation (79). Kan^r transformants were recovered on brain heart infusion (BHI; BD Difco)-TV-Kan plates and confirmed by PCR and sequencing. The Δ*kpsM* 81-176 capsule export mutant was a generous gift from Patricia Guerry (7).

Construction of a *C. jejuni* Tn*7*-based Tn library. A commercially available Tn*7*-based in vitro mutagenesis system (GPS-M; New England Biolabs), previously modified for use in *Helicobacter pylori* (64), was used to mutagenize *C. jejuni.* The previously described pGPS-cat vector harboring the Cm acetyltransferase gene (CAT) and purified transposase enzyme from New England Biolabs were used according to the manufacturer's instructions to mutagenize *C. jejuni* 81-176 chromosomal DNA, which was purified by two CsCl gradient centrifugations (5). This mutagenized DNA was transformed into *C. jejuni* 81-176 by natural transformation and electroporation (79), and Cm-resistant clones were selected on MH-TV-Cm plates. Approximately 1,000 single colonies were directly harvested from the plates and stored at −80°C; 20 of the colonies were screened by Southern analyses to confirm random Tn*7* insertion (data not shown). This now represents the fourth method for in vitro transposon (Tn) mutagenesis of *C. jejuni* (16, 27, 32).

CFW *dim* mutant screen. A 2% CFW M2R (Sigma fluorescent brightener 28) stock solution was prepared by diluting CFW in distilled water and adding 10 M NaOH drop-wise until the CFW dissolved (~15 μl NaOH/1 ml CFW); then it was filter sterilized and stored at 4°C in the dark. To screen for *dim* (CFW-hypofluorescent/hyporeactive) mutants, the Tn*7* library was grown for ~7 h microaerobically at 37°C on MH plates, the bacteria were harvested and diluted to ~2,000 CFU/ml, and 100-μl aliquots were spread on BHI-TV-0.002% CFW plates. The plates were incubated microaerobically at 37°C for 48 h and then transferred to a 42°C anaerobic environment for 24 h. All CFW plate growth and incubations were performed in the dark. CFW reactivity was visualized under long-wave (365 nm) UV light, and colonies exhibiting a hypofluorescent (dim) phenotype were selected and purified.

Molecular and genetic characterization of the *dim* mutants. To identify the Tn insert site in *dim10*, three procedures were employed. The first was an inverse PCR approach: genomic DNA was digested with either HindIII or ClaI, fragments were circularized by ligation, and PCR was performed using S+H3down or N+H3up primers (Table 1). The S+H3down reaction yielded part of the 81-176 intergenic region shown below (see Fig. 2) plus a short fragment of Cj0967, but the N+H3up reactions were unsuccessful. We next attempted a random prime approach described in the work of Salama et al. (64). Again, the S primer reactions yielded part of Cj0967 and the 81-176-specific intergenic region, but no product was obtained for the N side of the Tn. PCR amplification of the Cj0965c-Cj0967 region of the WT and the *dim10* mutant yielded identical

sequences, indicating that the Tn was not at this locus. Therefore, we digested *dim10* mutant genomic DNA with BclI to yield predicted ~5- to 15-kb fragments, which were ligated into pUC18 cut with BamHI. Positive *E. coli* clones were identified using Cm, and the entire clone was sequenced. Southern analyses performed on 81-176 WT and the *dim10* mutant and 11168 WT DNA by use of Cj0967 as a probe confirmed the presence of two Cj0967-Cj0975 loci in 81-176 and that the Tn had inserted at the second locus, upstream of Cj0967 and downstream of Cj0500.

The *dim13* Tn insertion was mapped by HindIII digestion of genomic DNA followed by circularization and inverse PCR with S+H3down or N+H3up primers, yielding sequences both up- and downstream of the Tn insert. To transform the *dim13* Tn insert into a clean WT background, ~1 μg of *dim13* genomic DNA was introduced into 81-176 by natural transformation, and Cm-resistant clones were selected on MH-TV-Cm plates. Δ*spoT dim10* and Δ*spoT dim13* double mutants were constructed by transforming Δ*spoT* genomic DNA into the *dim10* and *dim13* mutants and selecting on MH-TV-Cm-Kan plates. To construct a targeted *carB* deletion strain, ~500 bp from both the 5′- and 3′-most ends of *carB* were amplified from 81-176 genomic DNA by use of primers carB-4fL1, carB-4fR1, carB-4fL2, and carB-4fR2 (Table 1) to introduce XhoI/EcoRI sites to the 5′region and BamHI/SacI sites to the 3′ region of *carB.* The *carB* amplicons were digested with the enzymes noted above, the Kan^r cassette was digested with EcoRI/BamHI, pBluescript was digested with XhoI/SacI, and the four fragments were ligated to generate a Δ*carB*::Kan^r disruption construct. Kan^r *C. jejuni* colonies were isolated following electroporation of the construct into 81-176 and selection on MH-TV-Kan plates. Primers annealing outside the region initially amplified were used to confirm the proper insertion of the *carB*::Kan^r disruption construct.

Bacterial growth and phenotype assays. *C. jejuni* strains grown for 8 h on MH plates were harvested in MH-TV broth, inoculated at an optical density at 600 nm (OD_{600}) of 0.002, and grown overnight in shaking broth culture to early log phase (~16 h). For general growth assays, cultures were diluted to an OD_{600} of 0.05 and grown shaking for 48 h, and OD_{600} and CFU were determined at various time points. For serum sensitivity assays, bacteria were grown to early log phase and then diluted in phosphate-buffered saline (PBS) to ~2×10^5 CFU/ml. Bacteria (50 μl) were mixed 1:1 with a 20% solution of normal human serum or the same serum heat killed (HK serum) in PBS for 60 min at 65°C. After 60 min of incubation in a 37°C microaerobic environment, bacteria were plated for CFU enumeration. Percent survival was determined by dividing the number of CFU in 10% serum by the number of CFU in 10% HK serum. Experiments were performed in triplicate with three replicates. To assay CFW fluorescence, bacteria were grown overnight on MH plates, harvested with BHI broth, and diluted to an OD_{600} of 0.02, and 10-μl aliquots were spotted on BHI plates containing 0.002% CFW. Bacteria were grown at 37°C under microaerobic conditions for 24 h and then allowed to continue growing under 37°C microaerobic conditions or transferred to 42°C anaerobic conditions. Photographs were taken under a long-wave UV lamp in the dark with an Olympus C-5060 digital camera.

TEM negative staining. Overnight cultures were inoculated at an OD_{600} of 0.002 and grown microaerobically to early log phase, diluted to an OD_{600} of 0.005, grown shaking microaerobically for 24 h, and then fixed with 2.5% glutaraldehyde in 0.1 M cacodylate buffer, loaded onto Formvar carbon-coated grids, negatively stained with 0.5% uranyl acetate, and visualized by transmission electron microscopy (TEM).

Carbohydrate preparation, SDS-PAGE, DOC-PAGE, silver staining, and CFW staining analyses. *C. jejuni* strains were grown on MH agar for 48 h microaerobically and prepared based on the method of Hitchcock and Brown (33). Briefly, bacteria were harvested with PBS and diluted to an OD_{600} of 10 in 100 μl. An equal volume of 2× lysis buffer (4% sodium dodecyl sulfate [SDS], 8% β-mercaptoethanol, 20% glycerol, 0.125 M Tris [pH 6.8], 0.025% bromophenol blue) was added to the cell suspension, which was then heated at 95°C for 10 min. After the samples cooled to room temperature, 10 μl of 10-mg/ml proteinase K was added and samples were incubated overnight at 37°C or 55°C. Samples were then incubated at 65°C for 1 h or 95°C for 5 min and separated on 6 to 16% deoxycholate (DOC)-polyacrylamide gel electrophoresis (PAGE) (68), 4 to 16% SDS-PAGE, or 6 to 16% SDS-PAGE gradient gels followed by either silver staining or CFW staining. Bio-Rad Kaleidoscope markers were also loaded onto each gel. Silver staining was performed according to the method outlined by Tsai and Frasch (77), with modifications as per the work of St. Michael et al. (68). For CFW staining, the gel was shaken for 45 min in a 0.01% CFW-0.5 M Tris (pH 9.2) solution, followed by destaining in water for 3 h. A long-wave (365-nm) UV light was used to visualize CFW staining. This experiment was conducted three times with similar results.

CV biofilm assays. Eight-hour plate cultures of *C. jejuni* were inoculated into broth at an OD_{600} of 0.002, grown shaking overnight (16 h) to early log phase (OD_{600}, ~0.2 to 0.4), and diluted to an OD_{600} of 0.05. Sterile 96-well polyvinyl chloride plates, polystyrene plates, or borosilicate tubes were inoculated with 100 μl (96-well plates) or 1 ml (borosilicate tubes) of culture and placed in 37°C microaerobic conditions without agitation. After 24, 48, and 72 h, the cultures were stained by adding 25 μl (plates) or 250 μl (tubes) of crystal violet (CV) staining solution (1% CV in 95% ethanol) and incubating at room temperature for 15 min. The tubes were thoroughly rinsed with H_2O and visually assessed, and photographs were taken with an Olympus C-5060 digital camera. To quantify biofilms, 1.5 ml dimethyl sulfoxide (DMSO) was added to each tube, the mixture was incubated for 24 to 48 h to dissolve the CV, and absorbance at 570 nm was assessed.

SEM. *C. jejuni* biofilms were grown in borosilicate tubes as described above, with a glass coverslip standing upright in the culture. After 24, 48, or 72 h, the cover glass was removed and gently rinsed once in 0.1 M cacodylate buffer, and the biofilms were fixed (2.5% glutaraldehyde in 0.1 M cacodylate) for 1 h. Cover glasses containing the biofilms were processed and visualized using scanning electron microscopy (SEM).

CLSM. *C. jejuni* biofilms were grown in borosilicate tubes in the dark, as described above, with the addition of 30 μl FM4-64 stock (Molecular Probes) and 15 μl of 0.2% CFW solution to the cultures. Cover glass strips containing the biofilms were recovered from the cultures and placed directly into a Lab-Tek II chamber #1.5 German cover glass system containing BHI broth for visualization on an Olympus inverted confocal laser scanning microscope (CLSM) at the Department of Cellular and Physiological Sciences at UBC.

HR-MAS NMR spectroscopy. Cells were prepared and analyzed by high-resolution magic angle spinning (HR-MAS) nuclear magnetic resonance (NMR) spectroscopy as previously described (70).

RESULTS

***C. jejuni* CFW reactivity is increased in a Δ*spoT* mutant, under 42°C anaerobic conditions, and after extended growth; CFW reactivity is decreased in *dim* mutants.** A *C. jejuni* Δ*spoT* mutant incapable of mounting an SR was previously shown to be defective for several phenotypes yet unexpectedly survived other predicted stresses (26). To investigate whether surface carbohydrates might play a role in these surprising results, WT and Δ*spoT* strains were patched onto plates containing CFW, and CFW reactivity was assayed by observing bacterial fluorescence under long-wave UV light. After 48 h of microaerobic growth at 37°C, the Δ*spoT* mutant was significantly more fluorescent than WT (Fig. 1A). Although the Δ*spoT* mutant was consistently more fluorescent than WT, we also observed a notable increase in WT fluorescence upon a 24-h shift to 42°C anaerobic conditions (Fig. 1B) and during extended growth under 37°C microaerobic conditions (Fig. 1C). We next screened a pilot Tn*7*-based Tn library, constructed in a WT background as described in Materials and Methods, for mutants that failed to hyperfluoresce following the 24-h 42°C anaerobic induction. Several *dim* (CFW hypofluorescent/hyporeactive) mutants were isolated, two of which, the *dim10* and *dim13* mutants, were selected for further characterization. As Fig. 1C shows, *dim* mutant fluorescence was severely attenuated both under 42°C anaerobic conditions and for the first 72 h of 37°C microaerobic growth, with only minimal fluorescence appearing after 96 h.

***dim* mutant genetic analyses reveal genomic differences between strains 11168 and 81-176 and a role for *carB* in CFW reactivity.** To determine the location of the Tn insertions, genomic DNA was prepared from the *dim10* and *dim13* mutants, and three mapping techniques were employed as described in Materials and Methods. This revealed that both *dim10* and *dim13* harbor Tns in intergenic regions of the 81-176 genome. While mapping the *dim10* Tn insert site, we found that relative to the published strain 11168 genome sequence

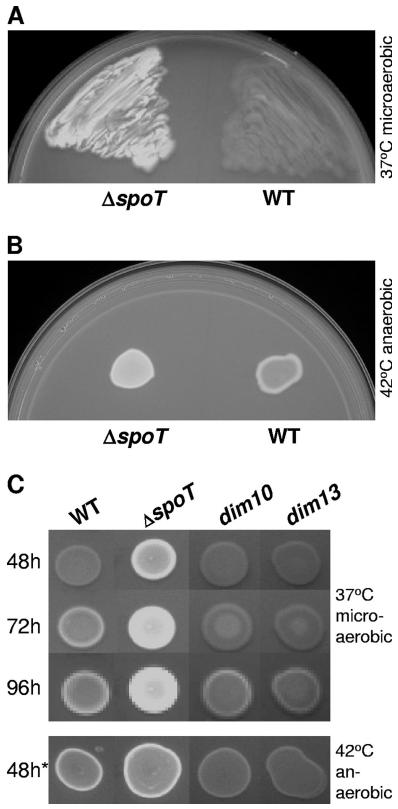

FIG. 1. CFW fluorescence phenotypes of 81-176 WT and Δ*spoT* and *dim* mutants visualized under long-wave UV light. (A and B) CFW reactivity profiles of WT versus the Δ*spoT* mutant. (A) WT and the Δ*spoT* mutant were patched onto BHI-CFW plates and grown for 48 h under 37°C microaerobic conditions. (B) Equal OD_{600} equivalents of WT and Δ*spoT* bacteria were spotted onto BHI-CFW plates and grown for 24 h under 37°C microaerobic conditions and then shifted for 24 h to 42°C anaerobic conditions. (C) Plate growth time course of CFW reactivity and *dim* mutant profiles compared to those of the WT and the Δ*spoT* mutant. Equal OD_{600} equivalents of WT and the Δ*spoT*, *dim10*, and *dim13* mutants were spotted onto BHI-CFW plates and grown for 48, 72, and 96 h under 37°C microaerobic conditions (top three rows) or for 24 h under 37°C microaerobic conditions followed by a 24-h incubation under 42°C anaerobic conditions (48h*). All CFW plate growth and incubation experiments were performed in the dark, and CFW reactivity was visualized by long-wave UV light. All strains were assayed on the same plate, although spot rearrangement was necessary for presentation purposes.

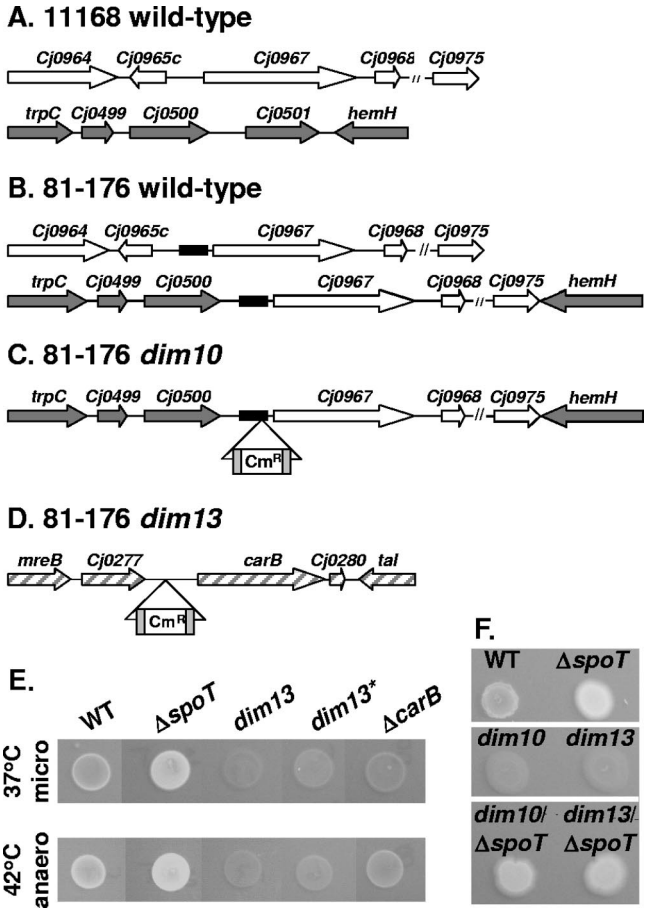

FIG. 2. Molecular and genetic analyses of *dim10* and *dim13* mutants. (A to D) Location of *dim10* and *dim13* Tn inserts and comparison of *dim10*-related sequences between WT 11168 and 81-176. (A) WT 11168: loci harboring the Cj0967 region (white arrows) and the Cj0500 region (dark gray arrows), based on published sequence data. (B) WT 81-176: two copies of the ~6-kb Cj0967-Cj0975 locus occur, one downstream of Cj0965c and one between Cj0500 and *hemH* (Cj0502). Cj0501 is absent in 81-176. A 200-bp 81-176-specific region of intergenic DNA is located upstream of Cj0967 at both loci (black boxes). (C) The *dim10* Tn insert (Cm^r flanked by gray boxes) maps within the 200-bp 81-176-specific intergenic region upstream of Cj0967 and downstream of Cj0500. Due to space constraints in panels A to C, two hatched lines (//) were used to represent DNA corresponding to the region between Cj0968 and Cj0975. (D) The *dim13* Tn insert (Cm^r flanked by gray boxes) maps upstream of *carB* (Cj0279) and downstream of Cj0277 in a region conserved between 11168 and 81-176 (hatched gray arrows). (E and F) Forty-eight-hour CFW plate assays on reconstructed *dim13* mutant (*dim13**) and *carB* targeted deletion (Δ*carB*) strains (37°C microaerobic and 42°C anaerobic analyses) (E) and on *dim10* Δ*spoT* and *dim13* Δ*spoT* double mutants (37°C microaerobic analysis) (F) were performed as described for Fig. 1. Although spot rearrangement for presentation purposes was necessary in panel E, for both panel E and panel F, all appropriate controls were included on the same plates as the test strains.

(60) (Fig. 2A), the WT 81-176 strain (Fig. 2B) contains two copies of an ~6-kb locus that begins ~300 bp upstream of Cj0967 and ends at the 3′ end of Cj0975. One copy occurs downstream of Cj0965c (Fig. 2B, top), while the second copy occurs between Cj0500 and *hemH* (Cj0502) (Fig. 2B, bottom). Cj0501 is absent from 81-176. Both copies of this locus in 81-176 also harbor an ~200-bp 81-176-specific region of intergenic DNA immediately upstream of Cj0967 (Fig. 2B). This region is >90% AT rich but contains an inverted repeat and a G-rich tract upstream of the Cj0967 start codon. The *dim10* Tn insert mapped within this 81-176-specific intergenic region (Fig. 2C), downstream of Cj0500 (encoding a putative ATP/GTP binding protein) and upstream of Cj0967 (encoding a putative periplasmic protein). The *dim13* Tn insert mapped to an intergenic region 80 bp downstream of Cj0277 (encoding a putative periplasmic protein with 30% identity to *H. pylori mreC*) and 181 bp upstream of *carB* (Cj0279) (encoding carbamoylphosphate synthase) in a region well conserved between 11168 and 81-176 (Fig. 2D).

We next wished to confirm that the dim phenotype of at least one of the mutants was due to the Tn insertion. Because of the diploid nature of the *dim10* insert site and the PCR recalci-

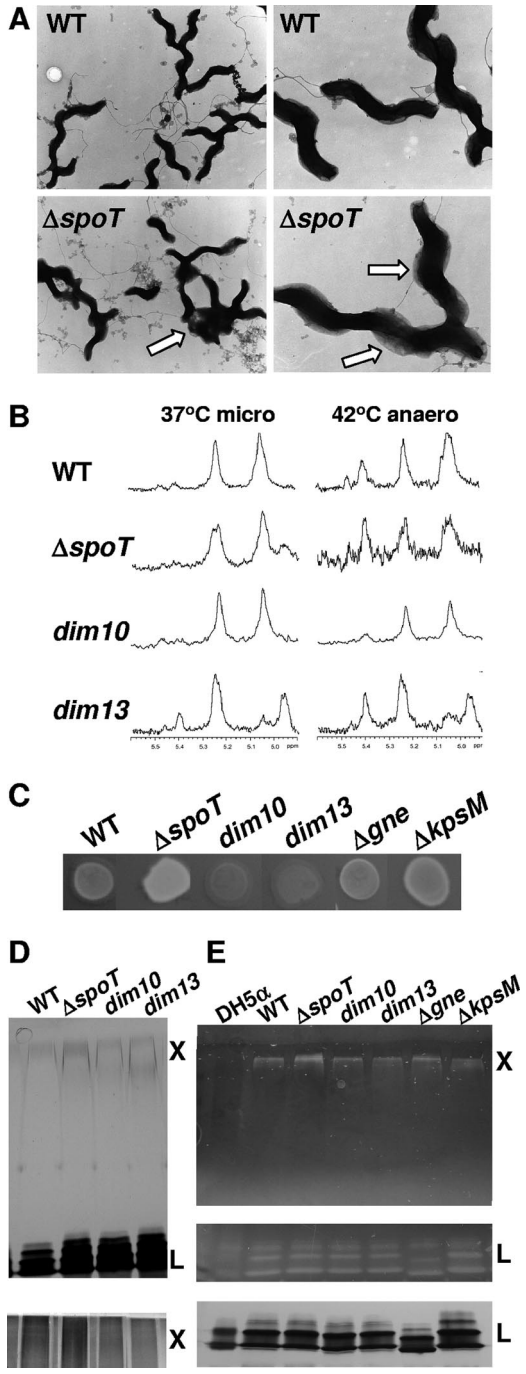

FIG. 3. Visual and biochemical investigations into the CFW-reactive polysaccharide by TEM, HR-MAS NMR, Δ*gne* and Δ*kpsM* CFW assays, and PAGE resolution followed by silver and CFW staining. (A) 81-176 WT and the Δ*spoT* mutant were grown microaerobically in liquid culture, fixed with glutaraldehyde, negatively stained with uranyl acetate, and visualized using TEM. The arrows point out exaggerated translucent surface material on the Δ*spoT* mutant and points of agglutination surrounded by the translucent material. (B) HR-MAS NMR spectra of 81-176 WT and Δ*spoT*, *dim10*, and *dim13* mutants showing the anomeric proton region which highlights the CPS resonances for bacteria grown for 48 h under 37°C microaerobic conditions or for 24 h under 37°C microaerobic conditions and then incubated for 24 h in 42°C anaerobic conditions. (C) CFW reactivity profiles of Δ*gne* and Δ*kpsM* mutants compared to those for relevant control strains grown on the same plate for 48 h under 37°C microaerobic conditions (as with Fig. 1 and 2, spot rearrangement was necessary for presentation purposes). (D) WT and Δ*spoT*, *dim10*, and *dim13* mutants were grown under 37°C microaerobic conditions for 48 h, polysaccharides were resolved by 4 to 16% SDS-PAGE (top) and 6 to 16% DOC-PAGE (bottom), and the gels were silver stained. "L" indicates LOS, and "X" indicates an uncharacterized high-MW polysaccharide that migrates just below the stacking gel and near or just above the 250-kDa Bio-Rad Kaleidoscope marker. (E) WT, the Δ*spoT*, *dim10*, *dim13*, Δ*gne*, and Δ*kpsM* mutants, and a control *E. coli* DH5α strain were grown as described for panel D, resolved by 4 to 16% (top) or 6 to 16% (middle and bottom) SDS-PAGE, and subjected to CFW staining (top and middle) or silver staining (bottom). Positions of the uncharacterized high-MW polysaccharide (X), running just below the stacking gel, and LOS are shown.

trance of the intergenic region upstream of Cj0967 (see Materials and Methods), we focused our efforts on *dim13*. First, *dim13* genomic DNA was used to transform the Tn insertion into a clean WT background. Multiple *dim13* transformants were recovered, a subset of which (represented by *dim13**) was confirmed by PCR. Second, a targeted *carB* deletion strain (the Δ*carB* strain) was generated and confirmed as described in Materials and Methods. Both the *dim13** and Δ*carB* strains exhibited a dim phenotype on CFW plates (Fig. 2E), confirming the linkage of the *dim13* mutation and implicating a role for *carB* in this phenotype.

Finally, to investigate dominance effects, double *dim10* Δ*spoT* and *dim13* Δ*spoT* mutants were constructed. Both of the double mutants were significantly brighter than WT on CFW plates, although slightly less bright than the Δ*spoT* mutant (Fig. 2F). The Δ*spoT* phenotype thus appears dominant, although some effect of the *dim* mutations on the Δ*spoT* mutant was observed.

CFW reactivity correlates with alterations in an uncharacterized *C. jejuni* polysaccharide. As CFW reacts with β1-3 and β1-4 carbohydrate linkages, we reasoned that differences in CFW reactivities likely represent differences in surface carbohydrate compositions. TEM analyses of glutaraldehyde-fixed WT and Δ*spoT* strains revealed a pronounced layer of translucent material coating the surface of Δ*spoT* bacteria that was less abundant in the WT strain (Fig. 3A). A high occurrence of cell-cell adhesion for the Δ*spoT* strain compared to that seen for WT was also observed, with adhesion points associated with the translucent surface material (Fig. 3A).

We next employed whole-cell HR-MAS NMR (37, 70) to analyze the CPS composition of WT, Δ*spoT*, *dim10*, and *dim13* strains grown on plates for 24 h under 37°C microaerobic conditions and then either maintained as such or transferred to 42°C anaerobic conditions for 24, 48, or 72 h. This revealed some differences between strains and incubation conditions; however, no clear signature correlating with CFW reactivity was identified (Fig. 3B), suggesting that the CFW-reactive polysaccharide does not correspond to the characterized *C. jejuni* CPS. For simplicity, only the anomeric regions showing the distinct CPS resonances (37) of 48-h samples are shown. However, the rest of the spectrum, including the β-anomeric region upfield from the HOD peak as well as spectra acquired at other time points, likewise revealed no clear signals correlating with CFW reactivity.

We next tested the CFW reactivities of two mutants known

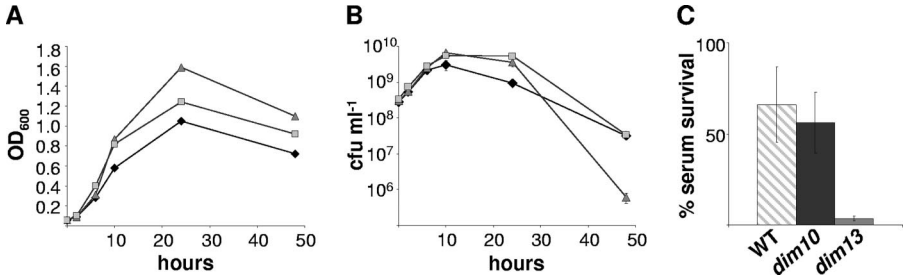

FIG. 4. Growth and survival of *dim* mutants in shaking broth culture and in the presence of human serum. (A and B) 81-176 WT (diamonds), the *dim10* mutant (triangles), and the *dim13* mutant (boxes) were grown in shaking MH broth culture, and OD_{600} (A) and CFU/ml (B) counts were taken at the indicated time points. Error bars are shown but are often too small to see. (C) Survival of WT, the *dim10* mutant, and the *dim13* mutant in human serum as measured by the ratio of CFU/ml recovered after 60 min in 10% normal human serum versus 10% HK human serum. $P < 0.0001$ for the *dim13* mutant versus the WT. No killing for any strain was observed in HK serum (not shown).

to be involved in the production of characterized *C. jejuni* polysaccharides. In strain 11168, *gne* encodes a bifunctional UDP-GlcNAc/Glc 4 epimerase involved in the synthesis of CPS, LOS, and *N*-linked carbohydrates (11); published structures of these polysaccharides suggest that each would also be affected in an 81-176 Δ*gne* mutant (3, 4, 86). KpsM is a conserved capsule transport protein, and Δ*kpsM* mutants fail to export the CPS in both 11168 and 81-176 (7, 38). Both 81-176 Δ*gne* and Δ*kpsM* mutants exhibited fluorescence levels similar to or slightly higher than that for WT on CFW plates under all conditions tested; for brevity, only 48-h 37°C microaerobic samples are shown (Fig. 3C).

Finally, to investigate the carbohydrate composition of these strains by gel electrophoresis, carbohydrates were prepared from WT and Δ*spoT*, *dim10*, and *dim13* mutants, resolved by 4 to 16% gradient SDS-PAGE or 6 to 16% gradient DOC-PAGE, and silver stained. This revealed a high-molecular-weight (MW) smear ("X") migrating at or just above the 250-kDa protein marker. This high-MW smear stained faintly in SDS gels (Fig. 3D, top) but stained more intensely in DOC gels (Fig. 3D, bottom) and reproducibly stained more intensely in Δ*spoT* samples and less intensely in *dim* mutant samples than WT. We next stained the gels directly with CFW. As DOC gels were incompatible with CFW staining, carbohydrates prepared from the above four strains, *E. coli* DH5α (as a negative control), and the Δ*gne* and Δ*kpsM* mutants were resolved by 4 to 16% and 6 to 16% SDS-PAGE to maximize the appearance of both "X" and the LOS and stained with CFW. This revealed that "X" reacted with CFW (Fig. 3E, top), that "X" from the Δ*spoT* mutant stained more intensely than that of any other strain, and that the *dim* mutants exhibited a decreased intensity of "X" compared to WT. "X" in the Δ*gne* and Δ*kpsM* mutants also reacted with CFW, while the DH5α control was blank. Not surprisingly, the LOS, which contains β1-3 and β1-4 linkages (29, 70), also reacted with CFW (Fig. 3E, middle). However, LOS staining levels were approximately equal for all strains assayed, and parallel silver staining of gels further supports the comparable levels of LOS among the strains (Fig. 3E, bottom). This analysis also demonstrated that *gne*, as predicted, affects LOS size in strain 81-176 (Fig. 3E, middle and bottom). The area between "X" and LOS, where CPS runs, did not react with CFW, nor were there any differences in CPS observed between WT, the Δ*spoT* mutant, and the *dim* mutants in immunoblots with Penner sera (data not shown). Together, these data indicate that the differences in CFW reactivity observed for the Δ*spoT* mutant, the WT, and the *dim* mutants may be due to an uncharacterized high-MW polysaccharide that occurs independently of both *gne*- and *kpsM*-affected structures.

***The dim* mutants exhibit growth differences compared to WT; the *dim13* mutant is serum sensitive.** We next wished to explore the biological implications of diminished CFW reactivity. The Δ*spoT* mutant was previously shown to exhibit defects in broth culture (26), and certain *C. jejuni* surface polysaccharide mutants exhibit decreased serum resistance (7, 28). We found that both *dim* mutants repeatedly achieved ~50%-higher log phase OD_{600} values (Fig. 4A) and ~4- to 6-fold-higher CFU/ml (Fig. 4B) than WT at 24 h of growth in broth culture. At 48 h, viability of the *dim10* mutant dramatically decreased (~17-fold), while the *dim13* mutant more closely resembled WT (Fig. 4B). Serum sensitivity was assayed by incubating standing broth cultures of early log phase WT and *dim10* and *dim13* mutants with either 10% human serum or 10% HK human serum. No survival defects were observed for any strain incubated with HK serum (data not shown). In contrast, *dim13* mutant survival was severely attenuated following exposure to 10% human serum (Fig. 4C). Shown are samples from a 60-min incubation; similar results were obtained at 40 and 80 min (data not shown). Notably, other tested attributes, including motility, plate growth, and salt, antimicrobial peptide, and bile stress susceptibility, were identical in *dim* mutants and in the WT (data not shown).

CV assays identify a correlation between CFW reactivity and biofilm formation. CFW-reactive polysaccharides from other bacteria have previously been linked to biofilm formation (47, 67). We first assayed biofilm formation in *C. jejuni* WT and Δ*spoT* and *dim* mutant strains by use of a well-characterized CV biofilm visualization technique (57). Equal bacterial loads were grown in borosilicate glass tubes, polyvinyl chloride plates, or polystyrene plates under microaerobic conditions at 37°C, standing without agitation, and biofilms that formed at the air-liquid interface were stained with CV. Similar results were obtained for all surfaces. Figure 5A shows photographs of representative CV-stained borosilicate glass tubes, while Fig. 5B shows a quantification of biofilms from triplicate borosilicate tubes following CV dissolution in DMSO and OD_{570} analyses. As with CFW reactivity, the Δ*spoT* mutant formed biofilms significantly more rapidly than WT, with clear biofilms

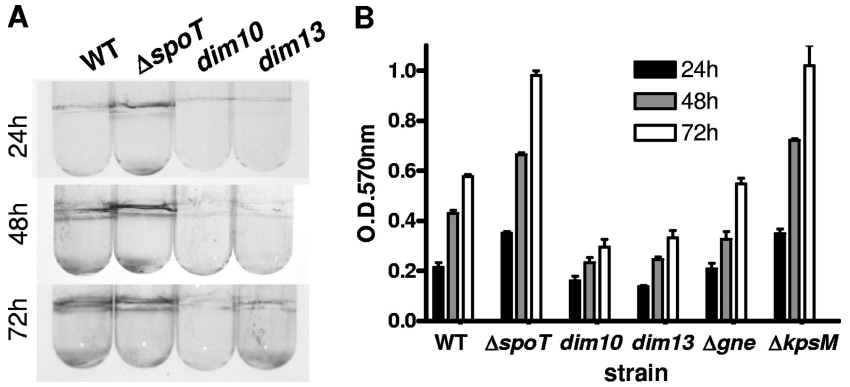

FIG. 5. CV staining of *C. jejuni* biofilms. (A) 81-176 WT and Δ*spoT*, *dim10*, and *dim13* mutants were incubated standing in broth for the indicated times under 37°C microaerobic conditions. Biofilms forming at the air-liquid interface were visualized by staining with 1% CV in 95% ethanol and photographed. (B) Biofilms of strains from panel A, as well as from Δ*gne* and Δ*kpsM* mutants, were grown in triplicate borosilicate tubes and stained with CV as described for panel A. CV was solubilized in DMSO, intensity was assessed by OD_{570} analyses, and data (with error bars) were graphed.

appearing after 24 h that increased over time. WT formed modest biofilms after 24 h and likewise exhibited increased biofilm formation over time. In contrast, the *dim* mutants, including the *dim13** mutant, were attenuated for biofilm formation (Fig. 5 and data not shown). As with CFW reactivity, biofilm formation was independent of *gne* and *kpsM*, with the Δ*gne* mutant forming biofilms similar to WT and the Δ*kpsM* mutant forming exaggerated biofilms (Fig. 5B).

SEM reveals three-dimensional (3-D) *C. jejuni* biofilm architecture that correlates with CFW reactivity. To corroborate the CV staining data, SEM was used to visualize biofilms from WT and the Δ*spoT*, *dim10*, and *dim13* mutants at the ultrastructural level (Fig. 6). Bacterial biofilms were grown microaerobically at 37°C on cover glass, fixed, and processed for SEM. Shown are 72-h samples; earlier time points confirm these data but did not contain enough adherent *dim* mutant bacteria to yield reasonable photos. The Δ*spoT* mutant formed very dense, thick biofilms with clear 3-D structure. Although less dense than those of the Δ*spoT* mutant, mature WT biofilms also developed. In contrast, the *dim* mutants were attenuated for biofilm formation, with small amounts of bacteria adhered to the glass surface and no visible biofilm structure.

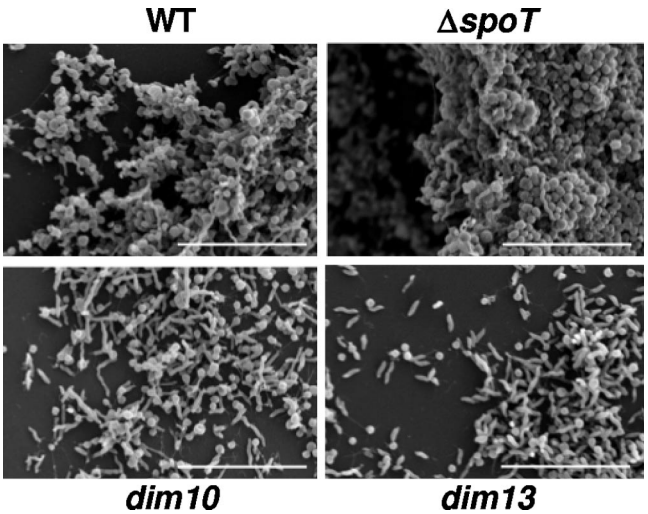

FIG. 6. SEM of biofilms formed after 72 h by 81-176 WT and Δ*spoT*, *dim10*, and *dim13* mutants. 81-176 WT and Δ*spoT*, *dim10*, and *dim13* mutant biofilms were grown on borosilicate cover glass in standing liquid cultures under 37°C microaerobic conditions for 72 h and visualized by SEM. Bars, 10 μm.

CLSM demonstrates native *C. jejuni* biofilm formation. As SEM entails harsh fixation procedures that usually result in the destruction of surface carbohydrates and extracellular polymeric substances, CLSM was used to visualize living WT and Δ*spoT*, *dim10*, and *dim13* mutant biofilms in a more native form (Fig. 7). Bacteria were grown on standing coverslips as described above, for 48 h, in the presence of two vital dyes: CFW (green) and FM4-64, a lipophilic dye that intercalates into the membrane (red). Shown in Fig. 7 are angled, top-down, and side profiles of the biofilms. These analyses revealed that WT formed thick biofilms with a clear 3-D structure. However, the Δ*spoT* mutant biofilms were more mature, with clear mushroom-like protrusions and much more pronounced 3-D architecture than seen for WT. In contrast, the *dim10* and *dim13* mutants were attenuated for biofilm formation.

DISCUSSION

C. jejuni is a highly prevalent human pathogen, yet our understanding of its survival, transmission, and pathogenesis strategies is limited. *C. jejuni*'s prevalence is also perplexing considering its fastidious growth and survival requirements during laboratory culture. We previously found that *C. jejuni* utilizes the SR to navigate some stressful conditions (26) but that complementary and independent stress survival mechanisms must exist. In this work, we have identified a role for a CFW-reactive polysaccharide in *C. jejuni* biofilm formation, particularly the up-regulation of biofilms observed for the Δ*spoT* SR mutant. Genetic and biochemical analyses suggest that this polysaccharide is distinct from other characterized surface polysaccharides and may utilize novel genes in its biosynthesis. This work also provides new insight into *C. jejuni* biofilm structure and formation which, given the organism's

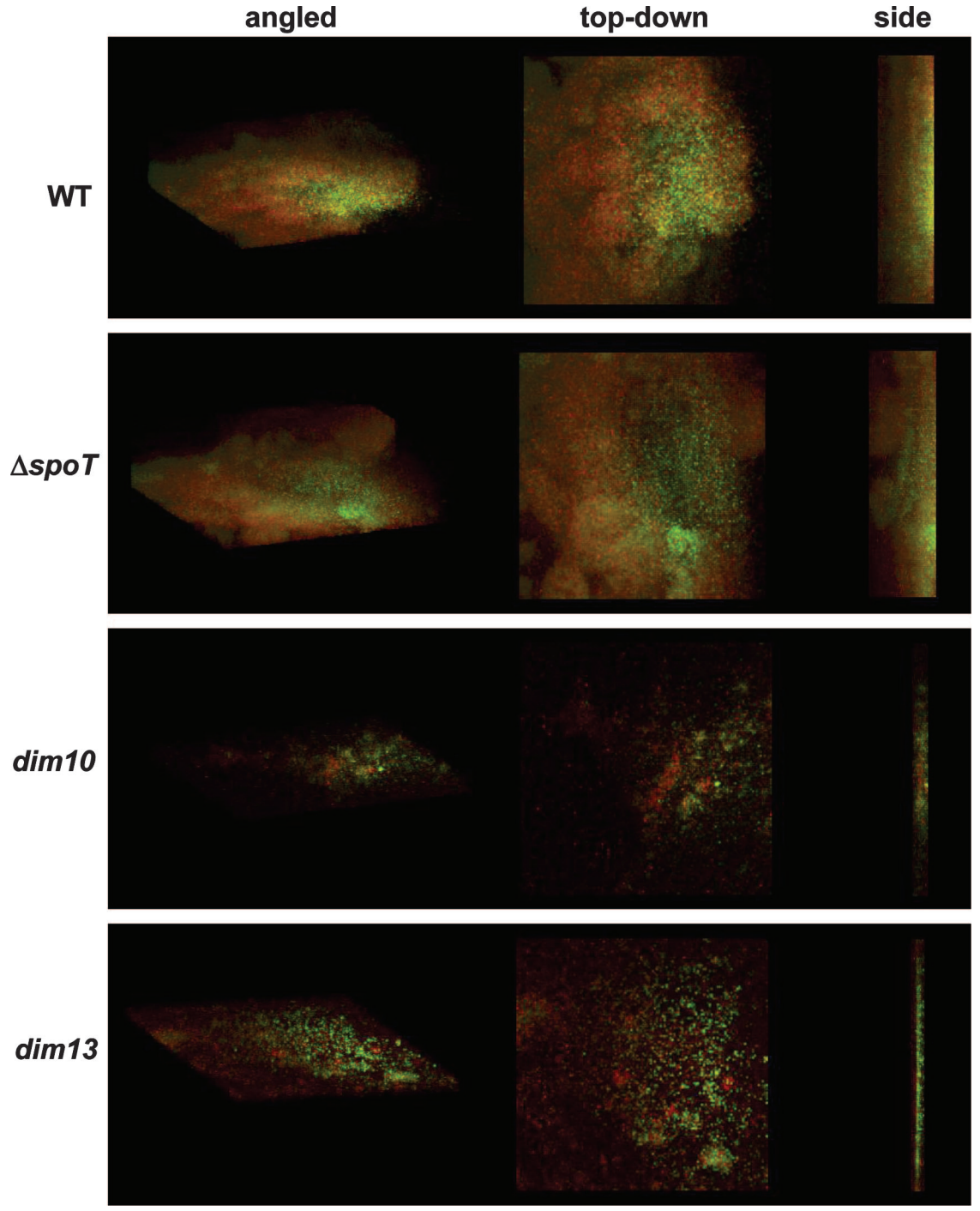

FIG. 7. CLSM of biofilms formed after 48 h by 81-176 WT and Δ*spoT*, *dim10*, and *dim13* mutants. 81-176 WT and Δ*spoT*, *dim10*, and *dim13* mutant biofilms were grown on borosilicate cover glass in standing liquid cultures under 37°C microaerobic conditions for 48 h in the presence of CFW and FM4-64 and visualized by CLSM. As noted at the top of the figure, angled, top-down, and side profiles are shown for each strain.

limited repertoire of hallmark stress response factors, is likely to be a major survival modality for *C. jejuni.*

CFW reactivity with *C. jejuni* has not previously been described. Our TEM, NMR, Δ*gne* and Δ*kpsM* mutant CFW assays, and PAGE analyses suggest that the CFW-reactive polysaccharide up-regulated in the Δ*spoT* mutant and down-regulated in the *dim* mutants is distinct from previously characterized CPS, LOS, and *N*-linked carbohydrates. Although the LOS bound CFW, its intensity in silver- and CFW-stained gels did not vary among our strains, nor was a Δ*gne* mutant with altered LOS defective for CFW reactivity. Instead, our data suggest that 81-176 produces a high-MW CFW-reactive polysaccharide with higher abundance in the Δ*spoT* mutant and lower abundance in the *dim* mutants. Previous studies

have also noted additional polysaccharides in strain 81-176. One, a novel cell surface α-glucan capsule, was shown by NMR to have an anomeric resonance of 5.4 ppm (58), which, together with another uncharacterized resonance at 5.25 ppm, was also observed in our earlier 81-176 NMR studies of CPS (37). A variably expressed resonance at 5.4 ppm and a resonance at 5.25 ppm are visible in the HR-MAS NMR spectra presented in this work but do not correlate with the CFW-reactive trend described. Other reports have identified a *kpsM*-independent ladder-like glycan (7) and a lipid-linked high-MW CPS-like polysaccharide (17) in 81-176. It is possible that either of these polysaccharides may correspond to our CFW-reactive carbohydrate, although our glycan "X" appears to migrate at a higher MW than the previously described polysaccharides.

Neither bioinformatics searches for genes involved in synthesizing CFW-reactive carbohydrates in other bacteria nor examination of microarray data comparing WT to the Δ*spoT* mutant (26) yielded insight into factors potentially involved in producing the *C. jejuni* CFW-reactive polysaccharide. However, our identification of the *dim13* mutant and subsequent analysis of a targeted *carB* mutant suggest that carbamoylphosphate synthase may participate in this biosynthetic pathway. Carbamoylphosphate is a precursor of both arginine and pyrimidine nucleotides, which in turn participate in the formation of nucleotide diphosphosugar precursors (i.e., UDP-glucose) that are primary substrates for numerous polysaccharides. A recent report also implicated *carAB* in EPS biosynthesis and growth stage transitions in the extremophile *Halomonas eurihalina* (43). Our *dim10* analyses suggest a role for the Cj0967 operon in the CFW fluorescence phenotype and revealed a duplication of the Cj0967 locus into a distinct region of the 81-176 chromosome. In the promoters of both Cj0967 loci, we also identified an ~200-bp sequence containing inverted repeats that may represent insertion sequences or potential hairpin loops. Interestingly, BLAST analyses revealed that the only other organisms harboring this sequence are two GBS-related *C. jejuni* strains. The 81-176 genome was also recently published, confirming our sequence data (34). Expanded *dim* mutant screens, additional biochemical analyses, expression studies using an 81-176 microarray, and studies of the numerous genes of unknown function in the *C. jejuni* CPS loci should provide future insight into genes involved in the synthesis of the CFW-reactive polysaccharide.

We have also established a correlation between the production of the CFW-reactive polysaccharide and biofilm formation for the strains used in this study. Multiple methods showed that as CFW reactivity increased (i.e., in the Δ*spoT* mutant and in the WT during extended growth), so did the complexity of the biofilm architecture. Conversely, the *dim* mutants were defective for forming biofilms and instead appeared enhanced for planktonic growth. *C. jejuni* exhibits some differences in biofilm formation from other bacteria (see the SR discussion below); nonetheless, we found that its biofilm progression follows the hallmark pattern of adherence, 2-D microcolony formation, and generation of complex 3-D communities. Although *C. jejuni* biofilm genetics and formation strategies are poorly understood, recent studies of targeted deletions in strain 11168 have begun to reveal genetic components involved in this process (35, 36, 63, 65). One such study found that 11168 biofilms formed normally in LOS (*neuB1*) and *N*-linked carbohydrate (*pglH*) mutants and were exaggerated in a *kpsM* mutant (35). This is consistent with our observations and with those obtained with other bacteria, where the biofilm matrix utilizes a high-MW EPS that is often independent of other surface polysaccharides (13, 24, 40, 45). Epidemiological studies have implicated a role for biofilms in *C. jejuni* environmental survival, survival on food surfaces, and in chicken flock transmission via water supply feeders (21, 76, 88). An in vivo role for biofilms has not yet been demonstrated for *C. jejuni*; however, the colonization competence of the Δ*spoT* mutant (26) together with our recent work exploring *ppk1* (polyphosphate kinase 1) (15) and other genes currently under investigation (unpublished observations) suggest that biofilms may also be important inside an animal host. As such, an expanded understanding of biofilms through genetic screens as presented here should provide new information regarding numerous aspects of *C. jejuni* pathogenesis.

Finally, our observations suggest that biofilm formation and the production of the CFW-reactive polysaccharide may represent important *C. jejuni* stress responses induced under adverse conditions such as those encountered during extended growth and in the absence of an SR. For instance, although *C. jejuni* stationary phase is typically associated with detrimental or poorly understood effects such as oxidative stress, peptidoglycan and metabolism changes, and conversion to coccoid and viable-but-nonculturable forms (31, 74, 75), it has recently been shown to elicit general increases and alterations in polysaccharide composition (18, 52), similar to observations for other bacteria (9, 14, 43). Our stress response hypothesis is also consistent with the *dim13* mutant serum sensitivity defect, the *dim10* mutant late-stage culturability defect (which may reflect rapid nutrient depletion and toxic metabolite production without concomitant up-regulation of the protective polysaccharide), and a recent study describing the altered expression of oxidative and stress response proteins in biofilm versus planktonic populations of *C. jejuni* 11168 (36). Our hypothesis is also consistent with biofilm up-regulation in the *C. jejuni* Δ*spoT* mutant, even though this is contrary to observations reported to date for other SR mutants (10, 30, 42, 71). One reason for this discrepancy may be that several of the previous studies were of gram-negative gammaproteobacteria, which often elicit SR effects via direct signaling through RpoS (6, 72, 78). *rpoS* is absent from epsilon- and alphaproteobacteria, including a succinoglycan-overproducing *Sinorhizobium meliloti* SR mutant (82), which is also predicted to overproduce biofilms (D. Wells, unpublished data). A working model to explain this is that the *C. jejuni* and *S. meliloti* ppGpp-minus mutants may be under constant stress and/or prematurely initiate responses necessary to cope with stationary phase. In the absence of a sigma factor like RpoS, this may invoke a regulatory switch to increase polysaccharide production and accelerate conversion to a protective biofilm community. It will be interesting to determine if other epsilonproteobacterial SR mutants (53) likewise up-regulate surface polysaccharides and/or biofilms and to explore the role of SR cofactors such as DksA in these phenomena.

In summary, this work provides insight into the connection between biofilms and stress responses in *C. jejuni*, suggests a role for a CFW-reactive polysaccharide in these processes, and

highlights subtleties yet to be elucidated regarding *C. jejuni*'s ability to survive in vivo and in nature. These data also underscore differences between *C. jejuni* and many model organisms characterized to date that may be applicable to other bacteria as well.

ACKNOWLEDGMENTS

We thank Marc Lamoureux for excellent technical assistance with the NMR studies, Patricia Guerry for the Δ*kpsM* mutant strain, I. Robert Nabi and Patrick Lajoie for assistance with confocal microscopy techniques, Olivia Champion for critically reading the manuscript, and the Gaynor and Szymanski labs for helpful discussions.

D.H.W. is supported by NIH F32 AI062004-2, E.F. is supported by a Canadian Institutes of Health Research postdoctoral fellowship, and S.L.S. is supported by a Natural Sciences and Engineering Research Council of Canada CGS-M traineeship. E.C.G. is supported by a Canada Research Chair award, the Michael Smith Foundation for Health Research, and a Burroughs Wellcome Fund Career Development Award in the Biomedical Sciences. This work was funded by Canadian Institutes of Health Research operating grant MOP-68981 to E.C.G.

REFERENCES

1. **Adak, G. K., S. M. Meakins, H. Yip, B. A. Lopman, and S. J. O'Brien.** 2005. Disease risks from foods, England and Wales, 1996-2000. Emerg. Infect. Dis. **11:**365–372.
2. **Altekruse, S. F., N. J. Stern, P. I. Fields, and D. L. Swerdlow.** 1999. Campylobacter jejuni—an emerging foodborne pathogen. Emerg. Infect. Dis. **5:**28–35.
3. **Aspinall, G. O., A. G. McDonald, and H. Pang.** 1992. Structures of the O chains from lipopolysaccharides of Campylobacter jejuni serotypes O:23 and O:36. Carbohydr. Res. **231:**13–30.
4. **Aspinall, G. O., A. G. McDonald, T. S. Raju, H. Pang, A. P. Moran, and J. L. Penner.** 1993. Chemical structures of the core regions of Campylobacter jejuni serotypes O:1, O:4, O:23, and O:36 lipopolysaccharides. Eur. J. Biochem. **213:**1017–1027.
5. **Ausubel, F. M., R. Brent, R. E. Kingston, D. D. Moore, J. G. Seidman, J. A. Smith, and K. Struhl (ed.).** 1995. Current protocols in molecular biology, Wiley Interscience, New York, NY.
6. **Bachman, M. A., and M. S. Swanson.** 2001. RpoS co-operates with other factors to induce Legionella pneumophila virulence in the stationary phase. Mol. Microbiol. **40:**1201–1214.
7. **Bacon, D. J., C. M. Szymanski, D. H. Burr, R. P. Silver, R. A. Alm, and P. Guerry.** 2001. A phase-variable capsule is involved in virulence of Campylobacter jejuni 81-176. Mol. Microbiol. **40:**769–777.
8. **Baker, J., M. D. Barton, and J. Lanser.** 1999. Campylobacter species in cats and dogs in South Australia. Aust. Vet. J. **77:**662–666.
9. **Bakholdina, S. I., I. N. Krasikova, and T. F. Solov'eva.** 2001. Effect of a culturing method and growth phase on composition of lipopolysaccharides in Yersinia pseudotuberculosis. Bioorg. Khim. **27:**151–155. (In Russian.)
10. **Balzer, G. J., and R. J. McLean.** 2002. The stringent response genes relA and spoT are important for Escherichia coli biofilms under slow-growth conditions. Can. J. Microbiol. **48:**675–680.
11. **Bernatchez, S., C. M. Szymanski, N. Ishiyama, J. Li, H. C. Jarrell, P. C. Lau, A. M. Berghuis, N. M. Young, and W. W. Wakarchuk.** 2005. A single bifunctional UDP-GlcNAc/Glc 4-epimerase supports the synthesis of three cell surface glycoconjugates in Campylobacter jejuni. J. Biol. Chem. **280:**4792–4802.
12. **Blaser, M. J., D. N. Taylor, and R. A. Feldman.** 1983. Epidemiology of Campylobacter jejuni infections. Epidemiol. Rev. **5:**157–176.
13. **Branda, S. S., S. Vik, L. Friedman, and R. Kolter.** 2005. Biofilms: the matrix revisited. Trends Microbiol. **13:**20–26.
14. **Cadmus, M. C., L. K. Jackson, K. A. Burton, R. D. Plattner, and M. E. Slodki.** 1982. Biodegradation of xanthan gum by *Bacillus* sp. Appl. Environ. Microbiol. **44:**5–11.
15. **Candon, H. L., B. J. Allan, C. D. Fraley, and E. C. Gaynor.** 2007. Polyphosphate kinase is a pathogenesis determinant in *Campylobacter jejuni*. J. Bacteriol. **189:**8099–8108.
16. **Colegio, O. R., T. J. Griffin IV, N. D. Grindley, and J. E. Galan.** 2001. In vitro transposition system for efficient generation of random mutants of *Campylobacter jejuni*. J. Bacteriol. **183:**2384–2388.
17. **Corcoran, A. T., H. Annuk, and A. P. Moran.** 2006. The structure of the lipid anchor of Campylobacter jejuni polysaccharide. FEMS Microbiol. Lett. **257:**228–235.
18. **Corcoran, A. T., and A. P. Moran.** 2007. Influence of growth conditions on diverse polysaccharide production by Campylobacter jejuni. FEMS Immunol. Med. Microbiol. **49:**124–132.
19. **Devane, M. L., C. Nicol, A. Ball, J. D. Klena, P. Scholes, J. A. Hudson, M. G. Baker, B. J. Gilpin, N. Garrett, and M. G. Savill.** 2005. The occurrence of Campylobacter subtypes in environmental reservoirs and potential transmission routes. J. Appl. Microbiol. **98:**980–990.
20. **Donlan, R. M.** 2002. Biofilms: microbial life on surfaces. Emerg. Infect. Dis. **8:**881–890.
21. **Dykes, G. A., B. Sampathkumar, and D. R. Korber.** 2003. Planktonic or biofilm growth affects survival, hydrophobicity and protein expression patterns of a pathogenic Campylobacter jejuni strain. Int. J. Food Microbiol. **89:**1–10.
22. **Eppinger, M., C. Baar, G. Raddatz, D. H. Huson, and S. C. Schuster.** 2004. Comparative analysis of four Campylobacterales. Nat. Rev. Microbiol. **2:**872–885.
23. **Fouts, D. E., E. F. Mongodin, R. E. Mandrell, W. G. Miller, D. A. Rasko, J. Ravel, L. M. Brinkac, R. T. DeBoy, C. T. Parker, S. C. Daugherty, R. J. Dodson, A. S. Durkin, R. Madupu, S. A. Sullivan, J. U. Shetty, M. A. Ayodeji, A. Shvartsbeyn, M. C. Schatz, J. H. Badger, C. M. Fraser, and K. E. Nelson.** 2005. Major structural differences and novel potential virulence mechanisms from the genomes of multiple campylobacter species. PLoS Biol. **3:**e15.
24. **Fux, C. A., J. W. Costerton, P. S. Stewart, and P. Stoodley.** 2005. Survival strategies of infectious biofilms. Trends Microbiol. **13:**34–40.
25. **Garcia-Medina, R., W. M. Dunne, P. K. Singh, and S. L. Brody.** 2005. *Pseudomonas aeruginosa* acquires biofilm-like properties within airway epithelial cells. Infect. Immun. **73:**8298–8305.
26. **Gaynor, E. C., D. H. Wells, J. K. MacKichan, and S. Falkow.** 2005. The Campylobacter jejuni stringent response controls specific stress survival and virulence-associated phenotypes. Mol. Microbiol. **56:**8–27.
27. **Golden, N. J., A. Camilli, and D. W. Acheson.** 2000. Random transposon mutagenesis of *Campylobacter jejuni*. Infect. Immun. **68:**5450–5453.
28. **Guerry, P., C. P. Ewing, T. E. Hickey, M. M. Prendergast, and A. P. Moran.** 2000. Sialylation of lipooligosaccharide cores affects immunogenicity and serum resistance of *Campylobacter jejuni*. Infect. Immun. **68:**6656–6662.
29. **Guerry, P., C. M. Szymanski, M. M. Prendergast, T. E. Hickey, C. P. Ewing, D. L. Pattarini, and A. P. Moran.** 2002. Phase variation of *Campylobacter jejuni* 81-176 lipooligosaccharide affects ganglioside mimicry and invasiveness in vitro. Infect. Immun. **70:**787–793.
30. **Harris, B. Z., D. Kaiser, and M. Singer.** 1998. The guanosine nucleotide (p)ppGpp initiates development and A-factor production in Myxococcus xanthus. Genes Dev. **12:**1022–1035.
31. **Harvey, P., and S. Leach.** 1998. Analysis of coccal cell formation by Campylobacter jejuni using continuous culture techniques, and the importance of oxidative stress. J. Appl. Microbiol. **85:**398–404.
32. **Hendrixson, D. R., and V. J. DiRita.** 2003. Transcription of sigma54-dependent but not sigma28-dependent flagellar genes in Campylobacter jejuni is associated with formation of the flagellar secretory apparatus. Mol. Microbiol. **50:**687–702.
33. **Hitchcock, P. J., and T. M. Brown.** 1983. Morphological heterogeneity among *Salmonella* lipopolysaccharide chemotypes in silver-stained polyacrylamide gels. J. Bacteriol. **154:**269–277.
34. **Hofreuter, D., J. Tsai, R. O. Watson, V. Novik, B. Altman, M. Benitez, C. Clark, C. Perbost, T. Jarvie, L. Du, and J. E. Galan.** 2006. Unique features of a highly pathogenic *Campylobacter jejuni* strain. Infect. Immun. **74:**4694–4707.
35. **Joshua, G. W., C. Guthrie-Irons, A. V. Karlyshev, and B. W. Wren.** 2006. Biofilm formation in Campylobacter jejuni. Microbiology **152:**387–396.
36. **Kalmokoff, M., P. Lanthier, T. L. Tremblay, M. Foss, P. C. Lau, G. Sanders, J. Austin, J. Kelly, and C. M. Szymanski.** 2006. Proteomic analysis of *Campylobacter jejuni* 11168 biofilms reveals a role for the motility complex in biofilm formation. J. Bacteriol. **188:**4312–4320.
37. **Karlyshev, A. V., O. L. Champion, C. Churcher, J. R. Brisson, H. C. Jarrell, M. Gilbert, D. Brochu, F. St. Michael, J. Li, W. W. Wakarchuk, I. Goodhead, M. Sanders, K. Stevens, B. White, J. Parkhill, B. W. Wren, and C. M. Szymanski.** 2005. Analysis of Campylobacter jejuni capsular loci reveals multiple mechanisms for the generation of structural diversity and the ability to form complex heptoses. Mol. Microbiol. **55:**90–103.
38. **Karlyshev, A. V., D. Linton, N. A. Gregson, A. J. Lastovica, and B. W. Wren.** 2000. Genetic and biochemical evidence of a Campylobacter jejuni capsular polysaccharide that accounts for Penner serotype specificity. Mol. Microbiol. **35:**529–541.
39. **Korlath, J. A., M. T. Osterholm, L. A. Judy, J. C. Forfang, and R. A. Robinson.** 1985. A point-source outbreak of campylobacteriosis associated with consumption of raw milk. J. Infect. Dis. **152:**592–596.
40. **Ledeboer, N. A., and B. D. Jones.** 2005. Exopolysaccharide sugars contribute to biofilm formation by *Salmonella enterica* serovar Typhimurium on HEp-2 cells and chicken intestinal epithelium. J. Bacteriol. **187:**3214–3226.
41. **Leigh, J. A., E. R. Signer, and G. C. Walker.** 1985. Exopolysaccharide-deficient mutants of Rhizobium meliloti that form ineffective nodules. Proc. Natl. Acad. Sci. USA **82:**6231–6235.
42. **Lemos, J. A., T. A. Brown, Jr., and R. A. Burne.** 2004. Effects of RelA on key virulence properties of planktonic and biofilm populations of *Streptococcus mutans*. Infect. Immun. **72:**1431–1440.
43. **Llamas, I., A. Suarez, E. Quesada, V. Bejar, and A. del Moral.** 2003. Iden-

tification and characterization of the carAB genes responsible for encoding carbamoylphosphate synthetase in Halomonas eurihalina. Extremophiles **7:**205–211.
44. **Mack, D., M. Nedelmann, A. Krokotsch, A. Schwarzkopf, J. Heesemann, and R. Laufs.** 1994. Characterization of transposon mutants of biofilm-producing *Staphylococcus epidermidis* impaired in the accumulative phase of biofilm production: genetic identification of a hexosamine-containing polysaccharide intercellular adhesin. Infect. Immun. **62:**3244–3253.
45. **Mah, T. F., and G. A. O'Toole.** 2001. Mechanisms of biofilm resistance to antimicrobial agents. Trends Microbiol. **9:**34–39.
46. **Maira-Litran, T., A. Kropec, C. Abeygunawardana, J. Joyce, G. Mark III, D. A. Goldmann, and G. B. Pier.** 2002. Immunochemical properties of the staphylococcal poly-*N*-acetylglucosamine surface polysaccharide. Infect. Immun. **70:**4433–4440.
47. **Matsukawa, M., and E. P. Greenberg.** 2004. Putative exopolysaccharide synthesis genes influence *Pseudomonas aeruginosa* biofilm development. J. Bacteriol. **186:**4449–4456.
48. **Meredith, T. C., U. Mamat, Z. Kaczynski, B. Lindner, O. Holst, and R. W. Woodard.** 2007. Modification of lipopolysaccharide with colanic acid (M-antigen) repeats in Escherichia coli. J. Biol. Chem. **282:**7790–7798.
49. **Merritt, A., R. Miles, and J. Bates.** 1999. An outbreak of Campylobacter enteritis on an island resort, north Queensland. Commun. Dis. Intell. **23:** 215–220.
50. **Miller, W. G., and R. E. Mandrell.** 2005. Prevalence of *Campylobacter* in the food and water supply: incidence, outbreaks, isolation, and detection, p. 156–188. *In* J. M. Ketley and M. E. Konkel (ed.), *Campylobacter*: molecular and cellular biology. Horizon Bioscience, Wymondham, Norfolk, United Kingdom.
51. **Mittenhuber, G.** 2001. Comparative genomics and evolution of genes encoding bacterial(p) ppGpp synthetases/hydrolases (the Rel, RelA and SpoT proteins). J. Mol. Microbiol. Biotechnol. **3:**585–600.
52. **Moen, B., A. Oust, O. Langsrud, N. Dorrell, G. L. Marsden, J. Hinds, A. Kohler, B. W. Wren, and K. Rudi.** 2005. Explorative multifactor approach for investigating global survival mechanisms of *Campylobacter jejuni* under environmental conditions. Appl. Environ. Microbiol. **71:**2086–2094.
53. **Mouery, K., B. A. Rader, E. C. Gaynor, and K. Guillemin.** 2006. The stringent response is required for *Helicobacter pylori* survival of stationary phase, exposure to acid, and aerobic shock. J. Bacteriol. **188:**5494–5500.
54. **Nachamkin, I.** 2002. Chronic effects of Campylobacter infection. Microbes Infect. **4:**399–403.
55. **NIAID.** 2005. Fooborne diseases, health matters. http://www.niaid.nih.gov/factsheets/foodbornedis.htm. National Institutes of Health, Bethesda, MD.
56. **Okada, Y., S. Makino, T. Tobe, N. Okada, and S. Yamazaki.** 2002. Cloning of *rel* from *Listeria monocytogenes* as an osmotolerance involvement gene. Appl. Environ. Microbiol. **68:**1541–1547.
57. **O'Toole, G. A., and R. Kolter.** 1998. Initiation of biofilm formation in Pseudomonas fluorescens WCS365 proceeds via multiple, convergent signalling pathways: a genetic analysis. Mol. Microbiol. **28:**449–461.
58. **Papp-Szabo, E., M. I. Kanipes, P. Guerry, and M. A. Monteiro.** 2005. Cell-surface alpha-glucan in Campylobacter jejuni 81-176. Carbohydr. Res. **340:** 2218–2221.
59. **Parise, G., M. Mishra, Y. Itoh, T. Romeo, and R. Deora.** 2007. Role of a putative polysaccharide locus in *Bordetella* biofilm development. J. Bacteriol. **189:**750–760.
60. **Parkhill, J., B. W. Wren, K. Mungall, J. M. Ketley, C. Churcher, D. Basham, T. Chillingworth, R. M. Davies, T. Feltwell, S. Holroyd, K. Jagels, A. V. Karlyshev, S. Moule, M. J. Pallen, C. W. Penn, M. A. Quail, M. A. Rajandream, K. M. Rutherford, A. H. van Vliet, S. Whitehead, and B. G. Barrell.** 2000. The genome sequence of the food-borne pathogen Campylobacter jejuni reveals hypervariable sequences. Nature **403:**665–668.
61. **Primm, T. P., S. J. Anderson, V. Mizrahi, D. Avarbock, H. Rubin, and C. E. Barry III.** 2000. The stringent response of *Mycobacterium tuberculosis* is required for long-term survival. J. Bacteriol. **182:**4889–4898.
62. **Rattee, I. D., and M. M. Breur.** 1974. The physical chemistry of dye absorption, p. 180–182. Academic Press, New York, NY.
63. **Reeser, R. J., R. T. Medler, S. J. Billington, B. H. Jost, and L. A. Joens.** 2007. Characterization of *Campylobacter jejuni* biofilms under defined growth conditions. Appl. Environ. Microbiol. **73:**1908–1913.
64. **Salama, N. R., B. Shepherd, and S. Falkow.** 2004. Global transposon mutagenesis and essential gene analysis of *Helicobacter pylori*. J. Bacteriol. **186:**7926–7935.
65. **Sampathkumar, B., S. Napper, C. D. Carrillo, P. Willson, E. Taboada, J. H. Nash, A. A. Potter, L. A. Babiuk, and B. J. Allan.** 2006. Transcriptional and translational expression patterns associated with immobilized growth of Campylobacter jejuni. Microbiology **152:**567–577.
66. **Schmidt, M. A., L. W. Riley, and I. Benz.** 2003. Sweet new world: glycoproteins in bacterial pathogens. Trends Microbiol. **11:**554–561.
67. **Solano, C., B. Garcia, J. Valle, C. Berasain, J. M. Ghigo, C. Gamazo, and I. Lasa.** 2002. Genetic analysis of Salmonella enteritidis biofilm formation: critical role of cellulose. Mol. Microbiol. **43:**793–808.
68. **St. Michael, F., C. M. Szymanski, J. Li, K. H. Chan, N. H. Khieu, S. Larocque, W. W. Wakarchuk, J. R. Brisson, and M. A. Monteiro.** 2002. The structures of the lipooligosaccharide and capsule polysaccharide of Campylobacter jejuni genome sequenced strain NCTC 11168. Eur. J. Biochem. **269:**5119–5136.
69. **Szymanski, C. M., S. M. Logan, D. Linton, and B. W. Wren.** 2003. Campylobacter—a tale of two protein glycosylation systems. Trends Microbiol. **11:**233–238.
70. **Szymanski, C. M., F. S. Michael, H. C. Jarrell, J. Li, M. Gilbert, S. Larocque, E. Vinogradov, and J. R. Brisson.** 2003. Detection of conserved N-linked glycans and phase-variable lipooligosaccharides and capsules from Campylobacter cells by mass spectrometry and high resolution magic angle spinning NMR spectroscopy. J. Biol. Chem. **278:**24509–24520.
71. **Taylor, C. M., M. Beresford, H. A. Epton, D. C. Sigee, G. Shama, P. W. Andrew, and I. S. Roberts.** 2002. *Listeria monocytogenes relA* and *hpt* mutants are impaired in surface-attached growth and virulence. J. Bacteriol. **184:**621–628.
72. **Teich, A., S. Meyer, H. Y. Lin, L. Andersson, S. Enfors, and P. Neubauer.** 1999. Growth rate related concentration changes of the starvation response regulators sigmaS and ppGpp in glucose-limited fed-batch and continuous cultures of Escherichia coli. Biotechnol. Prog. **15:**123–129.
73. **Thibault, P., S. M. Logan, J. F. Kelly, J. R. Brisson, C. P. Ewing, T. J. Trust, and P. Guerry.** 2001. Identification of the carbohydrate moieties and glycosylation motifs in Campylobacter jejuni flagellin. J. Biol. Chem. **276:**34862–34870.
74. **Tholozan, J. L., J. M. Cappelier, J. P. Tissier, G. Delattre, and M. Federighi.** 1999. Physiological characterization of viable-but-nonculturable *Campylobacter jejuni* cells. Appl. Environ. Microbiol. **65:**1110–1116.
75. **Thomas, C., D. J. Hill, and M. Mabey.** 1999. Morphological changes of synchronized Campylobacter jejuni populations during growth in single phase liquid culture. Lett. Appl. Microbiol. **28:**194–198.
76. **Trachoo, N., J. F. Frank, and N. J. Stern.** 2002. Survival of Campylobacter jejuni in biofilms isolated from chicken houses. J. Food Prot. **65:**1110–1116.
77. **Tsai, C. M., and C. E. Frasch.** 1982. A sensitive silver stain for detecting lipopolysaccharides in polyacrylamide gels. Anal. Biochem. **119:**115–119.
78. **van Delden, C., R. Comte, and A. M. Bally.** 2001. Stringent response activates quorum sensing and modulates cell density-dependent gene expression in *Pseudomonas aeruginosa*. J. Bacteriol. **183:**5376–5384.
79. **van Vliet, A. H., K. G. Wooldridge, and J. M. Ketley.** 1998. Iron-responsive gene regulation in a *Campylobacter jejuni fur* mutant. J. Bacteriol. **180:**5291–5298.
80. **Wang, X., A. K. Dubey, K. Suzuki, C. S. Baker, P. Babitzke, and T. Romeo.** 2005. CsrA post-transcriptionally represses pgaABCD, responsible for synthesis of a biofilm polysaccharide adhesin of Escherichia coli. Mol. Microbiol. **56:**1648–1663.
81. **Wang, X., J. F. Preston III, and T. Romeo.** 2004. The pgaABCD locus of *Escherichia coli* promotes the synthesis of a polysaccharide adhesin required for biofilm formation. J. Bacteriol. **186:**2724–2734.
82. **Wells, D. H., and S. R. Long.** 2002. The Sinorhizobium meliloti stringent response affects multiple aspects of symbiosis. Mol. Microbiol. **43:**1115–1127.
83. **Wood, P. J.** 1980. Specificity in the interaction of direct dyes with polysaccharides. Carbohydr. Res. **85:**271–287.
84. **Workman, S. N., G. E. Mathison, and M. C. Lavoie.** 2005. Pet dogs and chicken meat as reservoirs of *Campylobacter* spp. in Barbados. J. Clin. Microbiol. **43:**2642–2650.
85. **Yohannes, K., P. Roche, C. Blumer, J. Spencer, A. Milton, C. Bunn, H. Gidding, M. Kirk, and T. Della-Porta.** 2004. Australia's notifiable diseases status, 2002: annual report of the National Notifiable Diseases Surveillance System. Commun. Dis. Intell. **28:**6–68.
86. **Young, N. M., J. R. Brisson, J. Kelly, D. C. Watson, L. Tessier, P. H. Lanthier, H. C. Jarrell, N. Cadotte, F. St. Michael, E. Aberg, and C. M. Szymanski.** 2002. Structure of the N-linked glycan present on multiple glycoproteins in the gram-negative bacterium, Campylobacter jejuni. J. Biol. Chem. **277:**42530–42539.
87. **Yuki, N., K. Susuki, M. Koga, Y. Nishimoto, M. Odaka, K. Hirata, K. Taguchi, T. Miyatake, K. Furukawa, T. Kobata, and M. Yamada.** 2004. Carbohydrate mimicry between human ganglioside GM1 and Campylobacter jejuni lipooligosaccharide causes Guillain-Barre syndrome. Proc. Natl. Acad. Sci. USA **101:**11404–11409.
88. **Zimmer, M., H. Barnhart, U. Idris, and M. D. Lee.** 2003. Detection of Campylobacter jejuni strains in the water lines of a commercial broiler house and their relationship to the strains that colonized the chickens. Avian Dis. **47:**101–107.
89. **Zogaj, X., M. Nimtz, M. Rohde, W. Bokranz, and U. Romling.** 2001. The multicellular morphotypes of Salmonella typhimurium and Escherichia coli produce cellulose as the second component of the extracellular matrix. Mol. Microbiol. **39:**1452–1463.